

---

# Thermodynamic analysis of the binding of component enzymes in the assembly of the pyruvate dehydrogenase multienzyme complex of *Bacillus stearothermophilus*

---

HYO-IL JUNG,<sup>1</sup> SIMON J. BOWDEN,<sup>1</sup> ALAN COOPER,<sup>2</sup> AND RICHARD N. PERHAM<sup>1</sup>

<sup>1</sup>Cambridge Centre for Molecular Recognition, Department of Biochemistry, University of Cambridge, Cambridge CB2 1GA, UK

<sup>2</sup>Department of Chemistry, University of Glasgow, Glasgow G12 8QQ, UK

(RECEIVED December 11, 2001; FINAL REVISION January 29, 2002; ACCEPTED January 29, 2002)

## Abstract

The peripheral subunit-binding domain (PSBD) of the dihydrolipoyl acetyltransferase (E2, EC 2.3.1.12) binds tightly but mutually exclusively to dihydrolipoyl dehydrogenase (E3, EC 1.8.1.4) and pyruvate decarboxylase (E1, EC 1.2.4.1) in the pyruvate dehydrogenase multienzyme complex of *Bacillus stearothermophilus*. Isothermal titration calorimetry (ITC) experiments demonstrated that the enthalpies of binding ( $\Delta H^\circ$ ) of both E3 and E1 with the PSBD varied with salt concentration, temperature, pH, and buffer composition. There is little significant difference in the free energies of binding ( $\Delta G^\circ = -12.6$  kcal/mol for E3 and  $= -12.9$  kcal/mol for E1 at pH 7.4 and 25°C). However, the association with E3 was characterized by a small, unfavorable enthalpy change ( $\Delta H^\circ = +2.2$  kcal/mol) and a large, positive entropy change ( $T\Delta S^\circ = +14.8$  kcal/mol), whereas that with E1 was accompanied by a favorable enthalpy change ( $\Delta H^\circ = -8.4$  kcal/mol) and a less positive entropy change ( $T\Delta S^\circ = +4.5$  kcal/mol). Values of  $\Delta C_p$  of  $-316$  cal/molK and  $-470$  cal/molK were obtained for the binding of E3 and E1, respectively. The value for E3 was not compatible with the  $\Delta C_p$  calculated from the nonpolar surface area buried in the crystal structure of the E3-PSBD complex. In this instance, a large negative  $\Delta C_p$  is not indicative of a classical hydrophobic interaction. In differential scanning calorimetry experiments, the midpoint melting temperature ( $T_m$ ) of E3 increased from 91°C to 97.1°C when it was bound to PSBD, and that of E1 increased from 65.2°C to 70.0°C. These high  $T_m$  values eliminate unfolding as a major source of the anomalous  $\Delta C_p$  effects at the temperatures (10–37°C) used for the ITC experiments.

**Keywords:** Pyruvate dehydrogenase; microcalorimetry; protein–protein interaction; thermodynamics; multienzyme complex

---

Reprint requests to: Professor R.N. Perham, Department of Biochemistry, University of Cambridge, 80 Tennis Court Road, Cambridge CB2 1GA, UK; e-mail: r.n.perham@bioc.cam.ac.uk; fax: 44(0)1223-333667.

**Abbreviations:** PDH, pyruvate dehydrogenase; E1, pyruvate decarboxylase (EC 1.2.4.1); E2, dihydrolipoyl acetyltransferase (EC 2.3.1.12); E3, dihydrolipoyl dehydrogenase (EC 1.8.1.4); PSBD, peripheral subunit-binding domain; LD, lipoyl domain; CD, catalytic domain; DD, di-domain; SPR, surface plasmon resonance; ITC, isothermal titration microcalorimetry; DSC, differential scanning calorimetry; HBS, Hepes buffered saline.

Article and publication are at <http://www.proteinscience.org/cgi/doi/10.1110/ps.4970102>.

The pyruvate dehydrogenase (PDH) complex is a member of a widespread family of multienzyme complexes responsible for the oxidative decarboxylation of 2-oxo acids, which have structural and mechanistic features in common (for reviews, see de Kok et al. 1998, Perham 2000, and references therein). The PDH complex ( $M_r = 5\text{--}10 \times 10^6$ ) is made up of multiple copies of three different enzymes, one of which, dihydrolipoyl acetyltransferase (E2, EC 2.3.1.12), self-assembles with either octagonal (24-mer) or icosahedral (60-mer) symmetry depending on the source, to

form the structural core of the complex. Multiple copies of the other two enzymes, pyruvate decarboxylase (E1, EC 1.2.4.1) and dihydrolipoyl dehydrogenase (E3, EC 1.8.1.4), bind tightly but independently to this E2 core.

The E2 polypeptide chain consists of several separately folded domains joined by extended, flexible linker regions. At the N-terminus are one or more lipoyl domains (up to three, again depending on the source of the E2 chain), each of which contains approximately 80 amino acid residues folded as an eight-stranded  $\beta$ -barrel. In each lipoyl domain is a lipoyl-lysine residue prominently displayed in an exposed  $\beta$ -turn, which acts as a 'swinging arm' in the swinging domain that serves to transfer the substrate between the three different active sites (Reed and Hackert 1990; de Kok et al. 1998; Jones et al. 2000; Perham 2000). Following the lipoyl domain(s) and linker regions is a much smaller domain (~35 amino acid residues) involved in binding the peripheral enzymes (E1 and E3), the structure of which is dominated by two parallel  $\alpha$ -helices connected by a loop region and a helical turn (Robien et al. 1992; Kalia et al. 1993). This peripheral subunit-binding domain (PSBD) in turn is separated by another linker region from the large (28kD) C-terminal domain that contains the acetyltransferase active site. It is this acetyltransferase domain that aggregates to form the inner structural core (octahedral or icosahedral) of the PDH complex (Reed and Hackert 1990; Perham 2000). The structures of the octahedral inner core of the *Azotobacter vinelandii* PDH complex (Mattevi et al. 1993) and the icosahedral inner core of the *Bacillus stearothermophilus* and *Enterococcus faecalis* PDH complexes (Izard et al. 1999) have been solved by means of X-ray crystallography.

In octahedral PDH complexes, the PSBD provides the binding site for E3, whereas E1 is thought to bind principally to the C-terminal acyltransferase domain (de Kok et al. 1998; Perham 2000). In contrast, the PSBD of the icosahedral PDH complex of *B. stearothermophilus* is responsible for binding both E1 and E3. The situation in the icosahedral PDH complexes of yeast and mammals is different again, owing to the presence of 6–12 copies of an additional type of subunit, protein X, in the E2 core (Sanderson et al. 1996). Protein X resembles the N-terminal half of the E2 chain, with a lipoyl domain capable of participating in PDH complex activity and a PSBD-like domain responsible for binding E3 (Patel and Roche 1990; Lawson et al. 1991). In such complexes it appears that the PSBD in the E2 chain binds only E1.

A recombinant di-domain (DD) representing the lipoyl domain and PSBD of the E2 chain of the *B. stearothermophilus* PDH complex is capable of binding to the dimeric E3 (Hipps et al. 1994) and tetrameric E1 ( $\alpha_2\beta_2$ ) (Lessard and Perham 1995) components from the same complex. In both instances, the stoichiometry of the interaction was surprisingly found to be 1:1, suggesting that the binding sites

for the PSBD on E1 and E3 must lie on, or close to, the two-fold axis of symmetry of the E3 dimer or E1 tetramer (Lessard and Perham 1995). The binding of *B. stearothermophilus* E3 and E1 to the PSBD is also mutually exclusive, but exhibits similar free energies ( $\Delta G_{\text{bind}}^\circ$ ) of  $-12.6$  and  $-12.9$  kcal/mol, respectively (Lessard et al. 1996) (Fig. 1A).

A crystal structure of the *B. stearothermophilus* E3-PSBD complex has revealed that the binding is dominated by electrostatic interactions between the negatively charged side chains of Asp and Glu residues derived from one E3 subunit, and positively charged side chains of Arg residues contributed by the PSBD (Mande et al. 1996). The binding site on E3 is indeed so close to the two-fold axis that the binding of one PSBD precludes the binding of a second (Fig. 1B). There is no crystal structure of *B. stearothermophilus* E1 or of the E1-PSBD complex. However, crystal structures of the homologous E1 ( $\alpha_2\beta_2$ ) components of *Pseudomonas putida* (Ævarsson et al. 1999a) and human (Ævarsson et al. 1999b) branched chain 2-oxo acid dehydrogenase complexes are available. Details of the binding site for PSBD on E1 are not clear, but biochemical studies indicate that the E1 $\beta$  subunit is chiefly responsible (Stepp and Reed 1985; Lessard and Perham 1995).

Recent advances in biological microcalorimetry have made it possible to explore directly, and in some detail, the thermodynamics of protein–protein interactions. In the present study, two calorimetric methods, isothermal titration calorimetry (ITC) and differential scanning calorimetry (DSC), were applied to determine the thermodynamic properties of the competitive interaction of E3 and E1 with the PSBD of *B. stearothermophilus* E2. The results have important general implications for protein–protein interaction when interpreted in the light of the E3-PSBD structure (Mande et al. 1996) and offer a deeper understanding of the assembly of this vast multifunctional enzyme complex.

## Results

### *Binding enthalpies of E3 and E1 with PSBD*

The heats of interaction of PSBD with E3 and E1 were determined using ITC. Figure 2 shows typical titrations for the interaction of DD with E3 and E1 in HBS buffer (10 mM Hepes, 150 mM NaCl, 3.4 mM EDTA) at pH 7.4 and 25°C, conditions identical to those used for surface plasmon resonance (SPR) measurements of the binding constant ( $K_a$ ) (Lessard et al. 1996). Under these conditions, complexation of DD with E3 (Fig. 2A) was endothermic (positive peaks in the ITC output), saturating at a stoichiometry of roughly 1:1. In contrast, under the same conditions, binding of DD to E1 was exothermic, but exhibited the same stoichiometry.

Integrated heat data (Fig. 2B) yield differential thermal binding curves which may be analyzed by standard nonlinear regression methods to give estimates of the binding

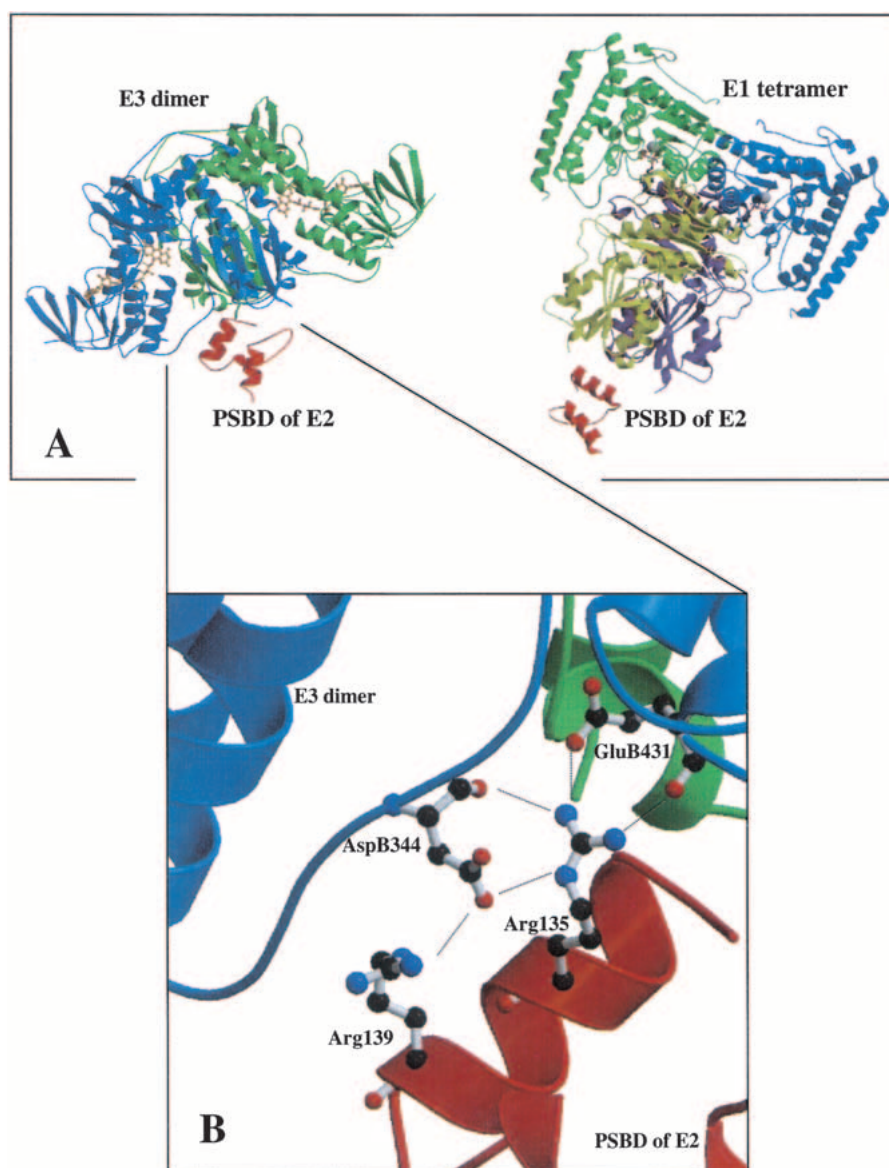


**Fig. 1.** (A) MolScript (Kraulis 1991) representation of the competitive interaction between E3 (green, monomer A; blue, monomer B; orange and ball-and-stick model, cofactor FAD) and E1 (green and blue,  $\alpha$  subunits; yellow and purple,  $\beta$  subunits; gray sphere, magnesium ion; red ball-and-stick model, thiamin diphosphate) and the PSBD (red) of E2 in the *B. stearothermophilus* PDH complex. The crystal structure of the E3-PSBD at 2.6Å resolution is that of Mande et al. (1996). The structure of E1 from the *B. stearothermophilus* PDH complex is unknown, but crystal structures of the E1 components of *P. putida* and human branched chain 2-oxo acid dehydrogenase complexes have been reported (Ævarsson et al. 1999a,b). A three-dimensional model (H.I. Jung, H. Chauhan, M. Fries, and R.N. Perham, unpubl.) of the *B. stearothermophilus* E1 derived from homology modeling (Guex and Peitsch 1997) is displayed here; the orientation of the PSBD with respect to the E1 $\beta$  subunits is arbitrary. (B) The binding interface of the E3-PSBD complex (Mande et al. 1996) is shown in detail. The electrostatic 'zipper' is formed between acidic residues (AspB344 and GluB431) of E3 and basic residues (Arg135 and Arg139) of the PSBD.

stoichiometry ( $n$ ), equilibrium constant for association ( $K_a$ ), and enthalpy of binding ( $\Delta H$ ), assuming a single stoichiometric binding equilibrium. However, as shown in a previous study using SPR detection (Lessard et al. 1996), the binding of DD to E3 and E1 is very tight ( $K_a = 1.7 \times 10^9 \text{ M}^{-1}$  for E3 and  $K_a = 3.1 \times 10^9 \text{ M}^{-1}$  for E1). For such tight

binding ( $K_a > 10^8 \text{ M}^{-1}$ ), only the enthalpy change upon binding ( $\Delta H$ ) and the stoichiometry of the association ( $n$ ) can be precisely determined by isothermal titration microcalorimetry (Wiseman et al. 1989). As shown in Fig. 2B, the binding stoichiometry calculated for each interaction was close to unity, which is in a good agreement with previous studies

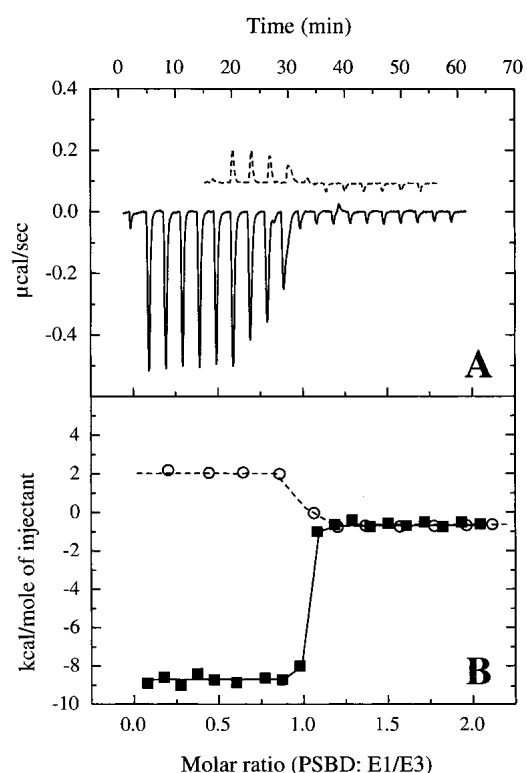


**Fig. 2.** Isothermal titration calorimetric analysis of the interaction of the PSBD (180–230 µM) with E3 (7.2 µM) and E1 (13.5 µM) components in HBS buffer (10 mM Hepes, 150 mM NaCl, and 3.4 mM EDTA, pH 7.4), at 25°C. (A) Raw data obtained over a series of injections of PSBD and plotted as heat (µcal/sec) versus time (min). Dashed line, binding of E3 showing the trace of positive peaks (endothermic); solid line, binding of E1 showing the trace of much larger negative peaks (exothermic). (B) Binding isotherms created by plotting the areas under the peaks in panel A against the molar ratio of the PSBD injected. The lines through the best-fit values obtained by least-squares regression using a one-site model give the stoichiometry ( $n$ ) and enthalpy ( $\Delta H$ ). For E3 (open circles and dashed line),  $n = 1.12$ ,  $\Delta H = +2.2$  kcal/mol; for E1 (closed rectangles and solid line),  $n = 0.98$  and  $\Delta H = -8.6$  kcal/mol.

(Hipps et al. 1994; Lessard et al. 1996; Mande et al. 1996). The binding enthalpies at 25°C were +2.2 and -8.4 kcal/mol for E3 and E1, respectively.

#### The effect of salt on the binding enthalpy

Previous kinetic measurements of the interaction of E1 and E3 with DD were performed in the presence of 150 mM NaCl to minimize any nonspecific binding during SPR detection (Lessard et al. 1996). To evaluate the effect of salt on the binding enthalpies, we titrated E1 and E3 with DD in the presence of four different concentrations of NaCl (up to 250 mM) at 30°C (Table 1). As the salt concentration was increased, the enthalpy of binding became less favorable, suggesting that charged groups play an important part in the interactions. In the case of E3, no heat of binding was ob-

served at higher salt concentrations ( $\geq 150$  mM) although the formation of an E3-DD complex under the same conditions was confirmed (data not shown) by means of non-denaturing PAGE (Lessard and Perham 1995). For experimental consistency and to allow comparison with other measurements, the concentration of the salt was fixed at 150 mM for further calorimetric measurements, unless stated otherwise.

#### E3 and E1 bind competitively to PSBD with different thermodynamic parameters

The standard free energy of binding ( $\Delta G^\circ$ ) was calculated from the equilibrium constant of the association ( $K_a$ ), determined previously by means of SPR analysis at 25 °C (Lessard et al. 1996), using the following expression:

$$\Delta G^\circ = -RT \ln K_a \quad (1)$$

The change of entropy on binding ( $T\Delta S^\circ$ ) was subsequently calculated from the relationship:

$$T\Delta S^\circ = \Delta H^\circ - \Delta G^\circ \quad (2)$$

where  $\Delta H^\circ$  is the enthalpy change of binding.

As shown in Table 2, the interaction of E3 with PSBD was found to be characterized by an enthalpically unfavorable ( $\Delta H^\circ = +2.2$  kcal/mol) but entropically favorable ( $T\Delta S^\circ = +14.8$  kcal/mol) process. In contrast, the enthalpy effect for E1 had the opposite sign to that for E3 under the same conditions, despite the small difference in the free energies of binding ( $\Delta G^\circ = -12.6$  kcal/mol for E3 and  $\Delta G^\circ = -12.9$  kcal/mol for E1). The association of E1 with PSBD was exothermic ( $\Delta H^\circ = -8.4$  kcal/mol), this strongly favorable enthalpy change being associated with an entropy change ( $T\Delta S^\circ$ ) of only +4.5 kcal/mol. These con-

**Table 1.** The enthalpy changes of the interaction of E3 and E1 with the PSBD at different temperatures and salt concentrations

pH	Temp. (°C)	Buffer	NaCl (mM)	Enthalpy change ( $\Delta H^\circ$ ) (kcal/mol)	
				E3	E1
7.4	30	Hepes	0	-7.7 ( $\pm 0.8$ )	-15.6 ( $\pm 1.2$ )
7.4	30	Hepes	50	-3.8 ( $\pm 0.4$ )	-13.3 ( $\pm 0.5$ )
7.4	30	Hepes	150	0*	-11.3 ( $\pm 0.0$ )
7.4	30	Hepes	250	0*	-10.2 ( $\pm 0.1$ )
7.4	10	HBS	150	+6.6 ( $\pm 0.6$ )	-1.7 ( $\pm 0.0$ )
7.4	25	HBS	150	+2.2 ( $\pm 0.1$ )	-8.4 ( $\pm 0.1$ )
7.4	30	HBS	150	0*	-11.3 ( $\pm 0.0$ )
7.4	37	HBS	150	-1.8 ( $\pm 0.3$ )	-14.3 ( $\pm 0.4$ )

All the values are the average of three or more repeated measurements, from which the standard error was calculated.

\* No heat change detected.

**Table 2.** Comparison of the thermodynamic parameters of the interaction of E3 and E1 with the PSBD of E2

Enzyme	$K_a^a$ ( $M^{-1}$ )	$\Delta G^{ob}$ (kcal/mol)	$\Delta H^{oc}$ (kcal/mol)	$T\Delta S^{od}$ (kcal/mol)	$\Delta C_p^c$ (kcal/molK)	Protons linked <sup>c</sup> (n)
E3	$1.7 \times 10^9$	-12.6	+2.2	+14.8	-316	-0.02
E1	$3.1 \times 10^9$	-12.9	-8.4	+4.5	-470	+0.11

All the kinetic and thermodynamic parameters are taken from experiments in HBS buffer, pH 7.4 at 25°C.

<sup>a</sup> Obtained from SPR analysis.

<sup>b</sup> Calculated from  $\Delta G^\circ = -RT \ln K_a$ .

<sup>c</sup> Calculated from ITC measurements.

<sup>d</sup> Calculated from  $T\Delta S^\circ = \Delta H^\circ - \Delta G^\circ$ .

trasting values exemplify, for E1 and E3, enthalpy–entropy compensation phenomena (Table 2) that now appear characteristic of many macromolecular interactions (Cooper et al. 2001).

#### Heat capacity changes

This apparent difference in thermodynamic signature (exothermic versus endothermic) between binding at 25°C becomes less clear cut when we consider the temperature dependence. Isothermal microcalorimetric titrations were carried out over a range of temperatures (10–37°C) in HBS buffer, pH 7.4, to obtain an estimate of heat capacity change,  $\Delta C_p$ , upon formation of the E3-PSBD and E1-PSBD complexes. This was derived from the slope of  $\Delta H^\circ$  versus T plots, assumed linear (Fig. 3), using the standard

thermodynamic relationship:

$$\Delta C_p = d \Delta H^\circ / dT \quad (3)$$

Both complexes showed a significant temperature dependence of  $\Delta H^\circ$  (Fig. 3), complex formation becoming more exothermic as the temperature rose. The data fit well to a linear function, whose slope gives the heat capacity change for binding of E1 or E3 to the PSBD. Values of  $\Delta C_p$  of  $-316$  ( $\pm 16$ ) cal/molK for E3 and  $-470$  ( $\pm 14$ ) cal/molK for E1 were obtained, which are around the average value ( $-333$  cal/molK) of  $\Delta C_p$  for protein–protein interactions (Stites 1997).

A large negative  $\Delta C_p$  has been thought to be characteristic of the classical hydrophobic interaction between non-polar groups in aqueous systems (Kauzmann 1959), and empirical correlations between  $\Delta C_p$  and changes in exposed surface area have been proposed (Spolar et al. 1992). From studies of model compounds (Murphy and Gill 1991), the change in heat capacity in a protein folding process was found to depend on buried polar and nonpolar surface area, according to the following empirical relationship (Murphy et al. 1993):

$$\Delta C_p = 0.45\Delta A_{np} - 0.26\Delta A_p \quad (4)$$

where  $\Delta A_{np}$  and  $\Delta A_p$  are the changes in the nonpolar and polar surface area buried upon folding, respectively. This relationship has been proposed to apply also to protein–protein interactions, as comparable with a folding process (Gómez and Freire 1995). Since a buried surface area has a negative sign in equation (4), a negative  $\Delta C_p$  is derived from the nonpolar buried surface area. Thus, a large negative  $\Delta C_p$  has been used as an indication of hydrophobic interaction in complex formation.

From the crystal structure of the E3-PSBD complex (Mande et al. 1996), the nonpolar and polar surface areas buried in the interface are  $674.9 \text{ \AA}^2$  and  $449.2 \text{ \AA}^2$ , respectively, calculated using the algorithm of Lee and Richards (1971) in the program NACCESS (Hubbard and Thornton 1993). Using equation (4), the calculated  $\Delta C_p$  is  $-187$  cal/

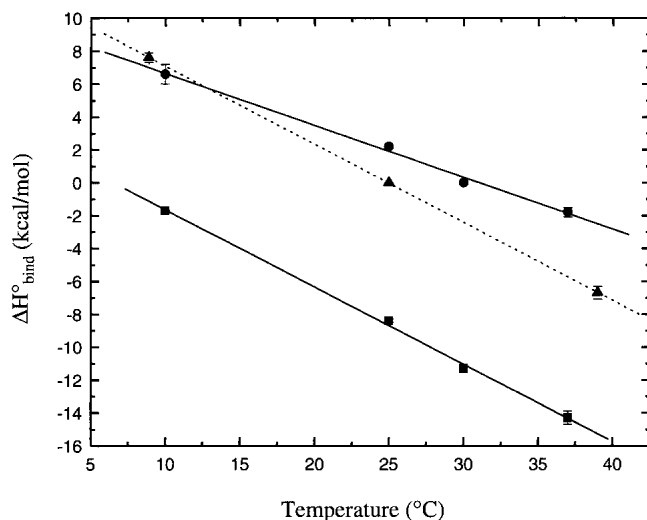


**Fig. 3.** Temperature dependence of enthalpy changes. The heat capacity ( $\Delta C_p$ ) values were determined from the slopes of the fitted lines. For E3 (closed circles and solid line),  $\Delta C_p = -316$  ( $\pm 16$ ) cal/molK; for E1 (closed rectangles and solid line),  $\Delta C_p = -470$  ( $\pm 14$ ) cal/molK in HBS buffer (10 mM Hepes, 150 mM NaCl, and 3.4 mM EDTA, pH 7.4). The dashed line (closed triangles) is for E3 in phosphate buffer (50 mM sodium phosphate, pH 7.0) without salt, giving  $\Delta C_p = -475$  ( $\pm 2$ ) cal/molK.

molK, significantly different from the value of  $-316$  cal/molK observed in the ITC measurements (see above). At lower ionic strength (50 mM sodium phosphate buffer, pH 7.0), an even greater temperature dependence of the heat of binding and, consequently, an even larger  $\Delta C_p$  ( $-475 \pm 2$  cal/molK), was observed (Fig. 3). Unless the separate E3 and PSBD and/or the E3-PSBD complex have markedly different conformations at different ionic strengths (for which there is no evidence), it is difficult to reconcile such  $\Delta C_p$  differences with changes in accessible surface area alone. The dependence of the absolute  $\Delta H$  values on ionic strength (Table 1, Fig. 3) indicate that electrostatic effects must be playing a significant role here. It is now becoming clear that large  $\Delta C_p$  effects, together with associated entropy–enthalpy compensations, are a much more general phenomenon to be anticipated in any system comprising a multiplicity of weak interactions (Dunitz 1995), and this has been quantitatively demonstrated in some systems (Cooper et al. 2001).

#### Protonation changes during complex formation

One possible source of anomalous enthalpy or heat capacity effects is uptake or release of protons during complexation (Stites 1997), and this can be examined by ITC experiments in different buffer systems (Bradshaw and Waksman 1998). For any process that embodies uptake or release of protons, the experimentally observed enthalpy change ( $\Delta H_{\text{obs}}$ ) will include contributions from the heat of protonation/deprotonation of the buffer employed. Thus it is essential that effects of buffer ionization ( $\Delta H_{\text{ion}}$ ) should be allowed for to obtain the true enthalpy change of binding ( $\Delta H_{\text{bind}}$ ). The relationship between these enthalpies is expressed by the following equation:

$$\Delta H_{\text{obs}} = \Delta H_{\text{bind}} + n\Delta H_{\text{ion}} \quad (5)$$

where  $n$  is the number of protons taken up (positive sign) or released (negative sign) by the buffer in the formation of the complex.

A further set of ITC experiments was therefore performed in several different buffers with different heats of ionization ( $\Delta H_{\text{ion}}$ ) and at four different pHs (pH 5.5, 6.5, 7.4, and 8.5). The enthalpies of ionization of the buffers used in this experiment were as follows: cacodylate,  $-0.56$  kcal/mol; MES,  $+3.73$  kcal/mol; Bistris,  $+6.75$  kcal/mol; Aces,  $+7.47$  kcal/mol; Hepes,  $+5.00$  kcal/mol; Tricine,  $+7.76$  kcal/mol; Tris-HCl,  $+11.51$  kcal/mol (Bradshaw and Waksman 1998). Experiments below pH 5.5 were not attempted, owing to the aggregation of both E3 and E1 in sodium acetate buffer at pH 4.5. The plots of  $\Delta H_{\text{obs}}$  versus  $\Delta H_{\text{ion}}$  for the formation of the E3-PSBD and E1-PSBD complexes are presented in Figure 4.

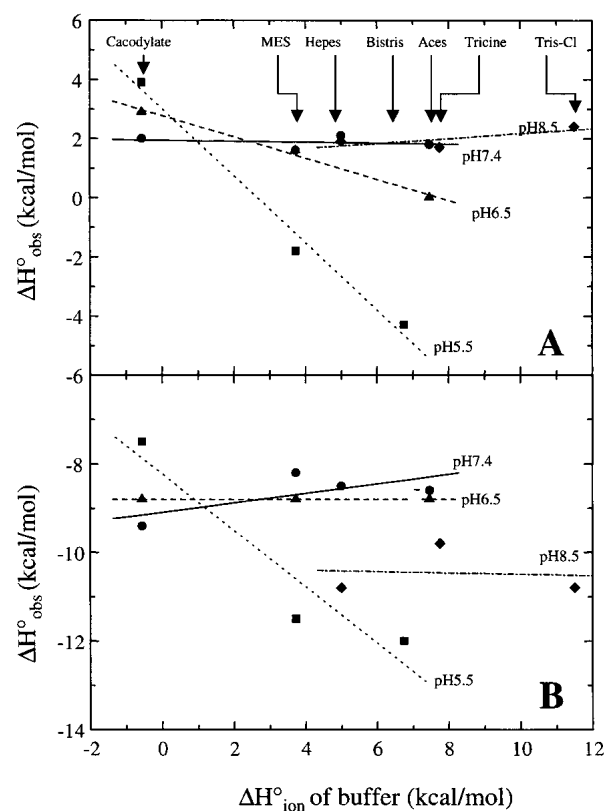


**Fig. 4.** Variation of the binding enthalpies ( $\Delta H^\circ$ ) for the interaction of E3 (A) and E1 (B) with PSBD as a function of the ionization enthalpy ( $\Delta H^\circ_{\text{ion}}$ ) of the buffer. All the experiments were at 25°C: pH 5.5 (■), pH 6.5 (▲), pH 7.4 (●) and pH 8.5 (◆). The average value of at least two estimates is depicted. Arrows indicate the  $\Delta H^\circ_{\text{ion}}$  values for the buffers employed. The number of protons linked to the complex formation is obtained from the slope of the best-fit line at a given pH.

Neither E3 nor E1 binding to PSBD showed significant protonation effects at pHs of 7.4 and 8.5, but there were clear buffer-dependent effects for the E3-PSBD complex at pH 6.5 and for both complexes at pH 5.5. The number of protons linked to the association event was obtained from the slope of the best-fit line at a specific pH. It appeared that there was release of up to one proton during binding to PSBD at acidic pH (Table 3). This suggests that one (or more) protein group(s) with acidic  $pK_a$  is (are) required in an unprotonated state for effective complex formation. Given the structural information about the E3-PSBD complex (Mande et al. 1996), the protonation observed in the E3-PSBD interaction may be due to two ionizable groups, Asp344 and Glu431, at the binding site on E3 (Fig. 1B). In the absence of a structure for E1-PSBD, it is impossible to speculate on the origins of any protonation effect there.

#### Thermal stability of the complexes

Anomalous  $\Delta C_p$  effects could also arise from perturbation of the protein structure, especially at temperatures close to

**Table 3.** The enthalpy changes of the interaction of E3 and E1 with PSBD in different buffers at different pH values

pH	Buffer	E3		E1	
		$\Delta H_{\text{obs}}^{\circ}$ (kcal/mol)	Protons linked <sup>a</sup> (n)	$\Delta H_{\text{obs}}^{\circ}$ (kcal/mol)	Protons linked <sup>a</sup> (n)
5.5	cacodylate	3.9	-1.14 ± 0.14	-7.5	-0.64 ± 0.21
	MES	-1.8		-11.5	
	Bistris	-4.3		-12.0	
6.5	cacodylate	2.9	-0.36 ± 0.04	-9.2	0.1 ± 0.01
	MES	1.6		-8.8	
	Aces	0		-8.4	
7.4	cacodylate	2.0	-0.02 ± 0.05	-9.4	0.11 ± 0.08
	MES	1.6		-8.2	
	Hepes	2.1		-8.5	
	Aces	1.8		-8.6	
8.5	Hepes	1.9	0.08 ± 0.07	-10.8	-0.02 ± 0.18
	Tricine	1.7		-9.8	
	Tris-HCl	2.4		-10.8	

All experiments were repeated twice and the average values are listed. The buffer conditions were 20 mM buffer, 150 mM NaCl and 3.4 mM EDTA at 25°C.

<sup>a</sup> The number of protons exchanged upon binding was obtained from the slopes of plots of  $\Delta H_{\text{obs}}$  versus  $\Delta H_{\text{ion}}$  in Figure 4.

the natural unfolding transition temperature,  $T_m$ . This possibility was tested by DSC experiments on the isolated E1 and E3 and their complexes with DD. Typical DSC curves are shown in Figure 5. Two distinct transitions were observed in a DSC experiment with DD alone, implying that

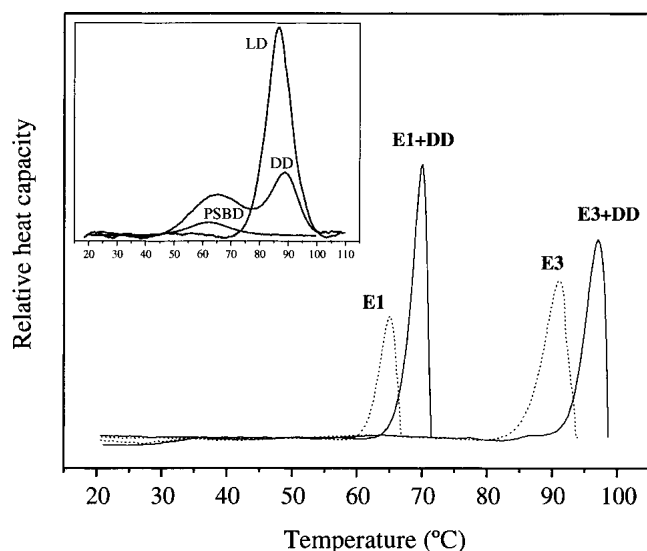


**Fig. 5.** DSC trace of the thermal denaturation of E3 ( $T_m = 91^\circ\text{C}$ ) and E1 ( $T_m = 65.2^\circ\text{C}$ ) in the absence (dotted line) and presence (solid line) of PSBD. *Inset*, DSC traces of the PSBD ( $T_m = 67.8^\circ\text{C}$ ), LD ( $T_m = 88.7^\circ\text{C}$ ), and DD.

the lipoyl domain and PSBD are unfolding independently, as expected for two domains linked by a long flexible segment of polypeptide chain. E1 and E3 were found to unfold in single cooperative transitions, with a  $T_m$  of  $91.0^\circ\text{C}$  and  $65.2^\circ\text{C}$  for E3 ( $3.6 \mu\text{M}$ ) and E1 ( $4.6 \mu\text{M}$ ), respectively. Both  $T_m$  values were shifted higher (to  $97.1^\circ\text{C}$  for E3 and  $70.0^\circ\text{C}$  for E1) in the presence of DD at a saturating concentration of  $22.3 \mu\text{M}$ , representing the enhanced thermal stability that accompanies tight complex formation in both instances. It is clear that no significant unfolding of E1, E3, or DD occurs at the much lower temperatures used for the ITC measurements, so perturbation of the protein structures is extremely unlikely as a major source of the anomalous  $\Delta C_p$  effects described above.

## Discussion

In general, an unfavorable enthalpy change and large positive entropy change associated with biomolecular complex formation might be characteristic of electrostatic (Ortiz-Salmerón et al. 1998) and/or hydrophobic interactions (Velazquez-Campoy et al. 2000). In the case of polar interactions such as hydrogen bonding, salt bridge formation, and other electrostatic effects, the unfavorable enthalpy change results from a net loss of such bonds, in forming the complex itself, or between ordered solvent molecules on the biomolecular surface. An unfavorable enthalpy change in hydrophobic interactions is due to the burial of hydrophobic groups, which also requires disruption of an ordered solvation network. In most hydrophobic interactions, the net enthalpy change is low and the entropy change is high. However, in both polar and hydrophobic interactions, most of the entropy gain is related to the liberation of water molecules from a binding interface in the course of complex formation, outweighing the loss of entropy associated with the formation of the complex itself. Consequently it is very difficult to disentangle the various components of molecular interactions from thermodynamic data alone (Cooper 1999; Cooper et al. 2001).

According to the  $2.6\text{\AA}$  crystal structure (Mande et al. 1996), the E3-PSBD complex is stabilized chiefly by electrostatic interactions between positively charged residues from the binding domain and negatively charged residues from the interface domains of both E3 monomers. Specifically, residues Arg135 and Arg139 of PSBD interact with Asp344 and Glu431 of E3 (monomer B), and no water molecule is visible in the binding interface (Fig. 1B). These charged sidechains of E3 and PSBD are likely to form hydration shells with water molecules when they are not in the complex. Thus, it appears that the thermodynamic parameters observed in the formation of the E3-PSBD complex reflect the presence of water molecules bound to the future binding site in the two proteins when they are uncomplexed

in solution and the release of such water molecules from the newly formed interface as the binding proceeds.

Other examples of water exclusion from interfaces caused by salt bridge formation can be found in biomolecular interactions such as protease–inhibitor, antigen–antibody and protein–DNA interactions (Janin 1999 and references therein). Many principles of molecular interaction have been developed from the fact that excluding water from mating surfaces can serve as a driving force in molecular association (Connelly et al. 1994; Ladbury 1996). Nevertheless, in some systems such as antibody–antigen interaction (Bhat et al. 1994), protein–carbohydrate interaction (Quiocho et al. 1989) and protein–peptide interaction (Tame et al. 1994), the inclusion of water appears to confer unusual specificity and enhanced affinity on the intermolecular interaction.

The source of heat capacity changes observed in protein–protein interactions is now becoming a subject of controversy. Various lines of evidence suggest that in an interaction mediated by a large number of water molecules, the retention of water molecules in a binding site can cause a significant contribution to the change in heat capacity upon binding (Morton and Ladbury 1996). There are also reports speculating that the burial of water in protein–protein interfaces is responsible for some of the negative changes in heat capacity (Bhat et al. 1994; Guinto and di Cera 1996; Stites 1997). A poor correlation between the measured and the calculated values for  $\Delta C_p$  in E3-PSBD complex formation casts doubt on the universality of the empirical relationship in equation (4) above and supports the suggestion that although the  $\Delta C_p$  for protein folding often correlates well with the burial of nonpolar surface, a similar correlation may not apply to protein–protein interactions (Raman et al. 1995).

The association of E3 with the PSBD would have been wrongly inferred as being governed by hydrophobic interactions, on the basis that it is entropy-driven. The *B. stearothermophilus* E3-PSBD complex must be added to the growing list of protein–protein interactions that show little, if any, correlation between  $\Delta C_p$  and the nonpolar surface area buried on binding (Raman et al. 1995; Pearce et al. 1996; Frisch et al. 1997). The large favorable enthalpy and small favorable entropy changes observed in the E1-PSBD interaction would normally be expected to imply more secondary forces, for example hydrogen bonds, as being involved, and less in the way of hydrophobic interactions between the two molecules. However, the strong component of electrostatic interaction in the E3-PSBD complex that we have seen to be associated with very different thermodynamic parameters makes it difficult to predict much with certainty about the interface in the E1-PSBD complex. A more detailed analysis of that binding interface will have to await a three-dimensional structure of the PSBD-complexed form of E1.

## Materials and methods

### Materials

All reagents used were of analytical grade. Unless otherwise indicated, buffers and chemicals were purchased from Sigma Chemicals. Bacteriological media were from Difco Laboratories. Ampicillin was purchased from Beecham Research. Restriction endonucleases *Bam*HI and *Nco*I were supplied by Pharmacia and New England Biolabs, respectively. The expression vector pET11d was supplied by Novagene. *Pfu* DNA polymerase and T4 DNA ligase were from Stratagene and Promega, respectively. Isopropyl-1-thio- $\beta$ -D-galactopyranoside (IPTG) was supplied by Melford Laboratory. *E. coli* strain JM 109 (*endA1*, *recA1*, *gyrA96*, *thi*, *hsdR17* (*rk<sup>-</sup>mk<sup>+</sup>*), *relA1*, *supE44*, *D(lac-proAB)*, [*F'*, *traD36*, *proAB*, *lacI<sup>q</sup>ZDM15*]) was used for genetic manipulations, and the lambda lysogen strain BL21(DE3), which carries the T7RNA polymerase gene under the control of the *lacUV5* promoter, was used for gene expression (Studier et al. 1990). HBS buffer (pH 7.4) is composed of 10 mM Hepes, 150 mM NaCl, and 3.4 mM EDTA.

### Construction of the plasmid pET11DD

The subgene encoding the DD (residues 1–170) of *B. stearothermophilus* E2 in the plasmid NAVDD (Hippis and Perham 1992) was amplified by polymerase chain reaction (PCR). The 21bp forward primer incorporated two mismatches to create an *Nco*I restriction site and to alter the translation initiation codon from GTG to ATG. Primer sequences were as follows: 5'-TAGAC AGACCATGGCTTTTGA-3' (forward, mismatches underlined) and 5'-ACCCGGGGATCCGTCGCCGC-3' (reverse). The resulting 573bp DNA fragment was treated with *Nco*I and *Bam*HI and purified by the “crush and soak” method (Maniatis et al. 1982) after electrophoresis in a 5% polyacrylamide gel. This fragment was then ligated into *Nco*I/*Bam*HI-cut, calf intestine alkaline phosphatase-treated pET11d. The resulting plasmid, pET11DD, was transformed into the *E. coli* strain JM 109 cells. The insert DNA was completely sequenced using the TagTrack™ Sequencing System (Promega) to check the fidelity of the PCR.

### Protein purification

*E. coli* BL21(DE3) cells transformed with pET11DD were grown at 37°C in 2 L of LB medium (Maniatis et al. 1982) supplemented with 50  $\mu$ g/mL ampicillin until the  $A_{600}$  was between 0.7 and 1.0. The cells were then induced with IPTG (final concentration of 1mM) and incubated for a further 2 h. The cells were harvested by centrifugation at 4,500  $\times g$  for 40 min, resuspended in 100 mM Tris-HCl buffer (pH 7.5) containing 1 mM EDTA, 0.02% sodium azide, 0.1 mM PMSF and disrupted in a French press at 4°C with cell pressure of 140 MPa. Cell debris was removed by ultracentrifugation at 20,000  $\times g$  for 20 min, and the supernatant was fractionally precipitated with solid ammonium sulphate (35%–70%). The protein in this fraction was subsequently dissolved in 10 mL of buffer A (20 mM potassium phosphate, pH 7.0, 0.02% sodium azide) and dialyzed overnight at 4°C against 2 L of the same buffer. The solution was then applied to a Pharmacia Hi-load™ S Sepharose column preequilibrated with buffer A and eluted with buffer B (20 mM potassium phosphate, pH 7.0, 0.02% sodium azide, 1M NaCl), applying a 15%–75% gradient over 4 column volumes at a flow rate of 1 mL/min. The fractions containing the DD (as judged by SDS-PAGE, apparent molecular mass 25 kD) were pooled, dialyzed again and loaded onto a Phar-

macia Mono™ Q high-performance anion-exchange column pre-equilibrated with buffer A. The protein was eluted with buffer B, again applying a 15%–75% gradient over 4 column volumes at a flow rate of 2 mL/min. Fractions containing the desired protein were pooled and concentrated by using Centriprep™ filtration. The recombinant E1 and E3 components were purified as described previously (Lessard and Perham 1994; Lessard et al. 1998). The purity of a protein during the purification process was monitored by means of SDS-PAGE using the Pharmacia Phast-System™. Protein solutions were prepared by exhaustive dialysis at 4°C against a large excess of deionized water and then concentrated to approximately 4.1 mM for DD, 1.5 mM for E3, and 0.28 mM for E1.

### Isothermal titration calorimetry

ITC measurements were carried out over different temperature ranges (10–37°C) using MCS-ITC and VP-ITC titration calorimeters (MicroCal, Northampton, MA) to obtain enthalpy and heat capacity changes (Wiseman et al. 1989). All of the protein samples for microcalorimetry were highly concentrated and then exhaustively dialyzed against deionized water. They were diluted into the various different buffers before the titration experiments, to minimize mixing heat effects caused by differences in solution composition. Diluted protein samples were then briefly but gently degassed before being added to the calorimeter cell. The DD, usually at a concentration of approximately 200  $\mu$ M, was injected in 10- $\mu$ L increments into the reaction cell (cell volume 1.31–1.41 mL) containing E3 at a concentration of around 7  $\mu$ M (or E1 at around 9  $\mu$ M) until complete saturation. A 250- $\mu$ L injection syringe with 310–400 rpm stirring was used to give a series of 10  $\mu$ L injections at 3-min intervals. Control experiments for heats of mixing and dilution were performed under identical conditions and used for data correction in subsequent analysis. Data acquisition and subsequent nonlinear regression analysis were done in terms of a simple binding model, using the Microcal ORIGIN software package.

### Differential scanning calorimetry

DSC measurements were carried out using a VP-DSC differential scanning calorimeter (Microcal) at a scan rate of 60°C/h in HBS buffer (10 mM Hepes, 150 mM NaCl, 3.4 mM EDTA, pH 7.4) (Cooper and Johnson 1994). Sample and reference solutions were gently degassed for approximately 3 min before loading into the cell. Samples were scanned from 20° to 110°C, but no re-scan was possible owing to the precipitation of denatured E3 and E1. DSC scans were corrected by subtraction of the data from suitable controls, and concentrations were normalized to determine the mid-point melting temperature ( $T_m$ ). The following concentrations were used for DSC experiments: approximately 50  $\mu$ M for DD, 10  $\mu$ M for PSBD, 340  $\mu$ M for lipoyl domain (LD), 3.0  $\mu$ M for E3, and 4.0  $\mu$ M for E1.

### General protein methods

Concentrations of protein samples were estimated from both amino acid analysis and UV absorbance measurements assuming  $A_{280}^{0.1\%} = 1.31$  (E3,  $M_r = 100,045$ ), 0.794 (E1,  $M_r = 153,333$ ), and 0.48 (DD,  $M_r = 18,383$ ) as reported (Hippis and Perham 1992; Lessard 1995). SDS-PAGE and amino acid analysis were carried out as described (Lessard 1995).

### Acknowledgments

This work was supported in part by a research grant (to R.N.P.) from the Biotechnology and Biological Sciences Research Council (BBSRC). We thank the BBSRC and the Wellcome Trust for their support of the core facilities in the Cambridge Centre for Molecular Recognition, and the BBSRC and Engineering and Physical Sciences Research Council for funding the biological microcalorimetry facilities in the University of Glasgow. We thank the Cambridge Overseas Trust and St John's College, Cambridge for financial support to H.I.J. We also thank C. Fuller, D. Pate, and M. Nutley for skilled technical assistance and Drs. G.J. Domingo and H.J. Chauhan for help with protein purification.

The publication costs of this article were defrayed in part by payment of page charges. This article must therefore be hereby marked "advertisement" in accordance with 18 USC section 1734 solely to indicate this fact.

### References

- Evarsson, A., Seger, K., Turley, S., Sokatch, J. R., and Hol, W.G.J. 1999a. Crystal structure of 2-oxoisovalerate dehydrogenase and the architecture of 2-oxo acid dehydrogenase multienzyme complexes. *Nat. Struct. Biol.* **6**: 785–792.
- Evarsson, A., Chuang, J.L., Wynn, R.M., Turley, S., Chuang, D.T., and Hol, W.G.J. 1999b. Crystal structure of human branched-chain  $\alpha$ -ketoacid dehydrogenase and the molecular basis of mutienzyme complex deficiency in maple syrup urine disease. *Structure* **8**: 277–291.
- Bhat, T.N., Bentley, G.A., Boulot, G., Greene, M.I., Tello, D., Dall'Acqua, W., Souchon, H., Schwarz, F.P., Mariuzza, R.A., and Poljak, R.J. 1994. Bound water molecules and conformational stabilization help mediate an antigen-antibody association. *Proc. Natl. Acad. Sci.* **91**: 1089–1093.
- Bradshaw, J.M. and Waksman, G. 1998. Calorimetric investigation of proton linkage by monitoring both the enthalpy and association constant of binding: Application to the interaction of the Src SH2 domain with a high-affinity tyrosyl phosphopeptide. *Biochemistry* **37**: 15400–15407.
- Connelly, P.R., Aldape, R.A., Bruzzese, F.J., Chambers, S.P., Fitzgibbon, M.J., Fleming, M.A., Itoh, S., Livingston, D.J., Navia, M.A., Thomson, J.A., and Wilson, K.P. 1994. Enthalpy of hydrogen bond formation in a protein-ligand binding reaction. *Proc. Natl. Acad. Sci.* **91**: 1964–1968.
- Cooper, A. 1999. Thermodynamic analysis of biomolecular interactions. *Curr. Opin. Chem. Biol.* **3**: 557–563.
- Cooper, A. and Johnson, C.M. 1994. Differential scanning calorimetry. In *Methods in molecular biology, Vol 22: Microscopy, optical spectroscopy and macroscopic techniques*. (eds. C. Jones, B. Mulloy, and A.H. Thomas A.H.), pp. 125–136. Humana Press; Totowa, NJ.
- Cooper, A., Johnson, C.M., Lakey, J.H., and Nöllmann, M. 2001. Heat does not come in different colours: Entropy–enthalpy compensation, free energy windows, quantum confinement, pressure perturbation calorimetry, solvation and the multiple causes of heat capacity effects in biomolecular interactions. *Biophys. Chem.* **28**: 215–230.
- de Kok, A., Hengeveld, A.F., Martin, A., and Westphal, A.H. 1998. The pyruvate dehydrogenase multienzyme complex from Gram-negative bacteria. *Biochim. Biophys. Acta* **1385**: 353–366.
- Dunitz, J.D. 1995. Win some, lose some—Enthalpy–entropy compensation in weak intermolecular interactions. *Chem. Biol.* **2**: 709–712.
- Frisch, C., Schreiber G., Johnson, C.M., and Fersht A.R. 1997. Thermodynamics of the interaction of barnase and barstar: Changes in free energy versus changes in enthalpy on mutation. *J. Mol. Biol.* **267**: 696–706.
- Gómez, J. and Freire, E. 1995. Thermodynamic mapping of the inhibitor site of the aspartic protease endothiapepsin. *J. Mol. Biol.* **252**: 337–350.
- Guex, N. and Peitsch, M.C. 1997. SWISS-MODEL and the Swiss-PdbViewer: An environment for comparative protein modelling. *Electrophoresis* **18**: 2714–2723.
- Guinto E.R. and di Cera, E. 1996. Large heat capacity change in a protein-monovalent cation interaction. *Biochemistry* **35**: 8800–8804.
- Hippis, D.S., Packman, L.C., Allen, M.D., Fuller, C., Sakaguchi, K., Appella, E., and Perham, R.N. 1994. The peripheral subunit-binding domain of the dihydrolipoyl acetyltransferase component of the pyruvate dehydrogenase complex of *Bacillus stearothermophilus*: Preparation and characterization of its binding to the dihydrolipoyl dehydrogenase component. *Biochem. J.* **297**: 137–143.

- Hipps, D.S. and Perham, R.N. 1992. Expression in *Escherichia coli* of a subgene encoding the lipoyl and peripheral subunit-binding domains of the dihydrolipoyl acetyltransferase component of the pyruvate dehydrogenase complex of *Bacillus stearothermophilus*. *Biochem. J.* **283**: 665–671.
- Hubbard, S.J. and Thornton, J.M. 1993. 'NACCESS', Computer Program, Department of Biochemistry and Molecular Biology, University College London. Further information can be found at <http://sjh.bi.umist.ac.uk/naccess.html>.
- Izard, T., Evarsson, A., Allen M.D., Westphal, A.H., Perham, R.N., de Kok, A., and Hol, W.G.J. 1999. Principles of quasi-equivalence and Euclidean geometry govern the assembly of cubic and dodecahedral cores of pyruvate dehydrogenase complexes. *Proc. Natl. Acad. Sci.*, **96**: 1240–1245.
- Janin J. 1999. Wet and dry interfaces: The role of solvent in protein–protein and protein–DNA recognition. *Structure* **7**: R277–R279.
- Jones, D.D., Stott, K.M., Howard, M.J., and Perham, R.N. 2000. Restricted motion of the lipoyl-lysine swinging arm in the pyruvate dehydrogenase complex of *Escherichia coli*. *Biochemistry* **39**: 8448–8459.
- Kalia, Y.N., Brocklehurst, S.M., Hipps, D.S., Appella, E., Sakaguchi, K., and Perham, R.N. 1993. The high-resolution structure of the peripheral subunit-binding domain of dihydrolipoamide acetyltransferase from the pyruvate dehydrogenase multienzyme complex of *Bacillus stearothermophilus*. *J. Mol. Biol.* **230**: 323–341.
- Kauzmann, W. 1959. Some factors in the interpretation of protein denaturation. *Adv. Protein Chem.* **14**: 1–63.
- Kraulis, P. 1991. MOLSCRIPT, a program to produce both detailed and schematic plots of protein structures. *J. Appl. Crystallog.* **24**: 946–950.
- Ladbury, J.E. 1996. Just add water! The effect of water on the specificity of protein-ligand binding sites and its potential application to drug design. *Chem. Biol.* **3**: 973–980.
- Lawson, J.E., Niu, X.-D., and Reed, L.J. 1991. Functional analysis of the domains of dihydrolipoamide acetyltransferase from *Saccharomyces cerevisiae*. *Biochemistry* **30**: 11249–11254.
- Lee, B.K. and Richards, F.M. 1971. Solvent accessibility of groups in proteins. *J. Mol. Biol.* **55**: 379–400.
- Lessard, I.A.D. 1995. "Protein–protein Interaction and Molecular Self-assembly of the Pyruvate Dehydrogenase Multienzyme Complex." PhD thesis, Department of Biochemistry, University of Cambridge, Cambridge, UK.
- Lessard, I.A.D., Fuller, C., and Perham, R.N. 1996. Competitive interaction of component enzymes with the peripheral subunit-binding domain of the pyruvate dehydrogenase multienzyme complex of *Bacillus stearothermophilus*: Kinetic analysis using surface plasmon resonance detection. *Biochemistry* **35**: 16863–16870.
- Lessard, I.A.D., Domingo, G.J., Borges, A., and Perham, R.N. 1998. Expression of genes encoding the E2 and E3 components of the *Bacillus stearothermophilus* pyruvate dehydrogenase complex and the stoichiometry of subunit interaction in assembly *in vitro*. *Eur. J. Biochem.* **258**: 491–501.
- Lessard, I.A.D. and Perham, R.N. 1994. Expression in *Escherichia coli* of genes encoding the E1 $\alpha$  and E1 $\beta$  subunits of the pyruvate dehydrogenase complex of *Bacillus stearothermophilus* and assembly of a functional E1 component ( $\alpha_2\beta_2$ ) *in vitro*. *J. Biol. Chem.* **269**: 10378–10383.
- Lessard, I.A.D. and Perham, R.N. 1995. Interaction of component enzymes with the peripheral subunit-binding domain of the pyruvate dehydrogenase multienzyme complex of *Bacillus stearothermophilus*: Stoichiometry and specificity in self-assembly. *Biochem. J.* **306**: 727–773.
- Mande, S. S., Sarfaty, S., Allen, M.D., Perham, R. N., and Hol, W.G.J. 1996. Protein–protein interactions in the pyruvate dehydrogenase multienzyme complex: Dihydrolipoamide dehydrogenase complexed with the binding domain of dihydrolipoamide acetyltransferase. *Structure* **4**: 277–286.
- Maniatis, T., Fritsch, E. F., and Sambrook, J. 1982. *Molecular cloning: A laboratory manual*, Cold Spring Harbor Laboratory Press, Cold Spring Harbor, NY.
- Mattevi, A., Obmolova, G., Kalk, K.H., Westphal, A.H., de Kok, A., and Hol, W.G.J. 1993. Refined crystal structure of the catalytic domain of dihydrolipoil transacetylase (E2p) from *Azotobacter vinelandii* at 2.6Å resolution. *J. Mol. Biol.* **230**: 1183–1199.
- Morton, C.J. and Ladbury, J.E. 1996. Water-mediated protein–DNA interactions: The relationship of thermodynamics to structural detail. *Protein Sci.* **5**: 2115–2113.
- Murphy, K.P. and Gill, S.J. 1991. Solid model compounds and the thermodynamics of protein unfolding. *J. Mol. Biol.* **222**: 699–709.
- Murphy, K.P., Xie, D., Garcia, K.C., Amzel, L.M., and Freire, E. 1993. Structural energetics of peptide recognition: Angiotensin II/antibody binding. *Proteins* **15**: 113–120.
- Ortiz-Salmerón, E., Barón, C., and García-Fuentes, L. 1998. Enthalpy of captopril-angiotensin I-converting enzyme binding. *FEBS Lett.* **435**: 219–224.
- Patel, M.S. and Roche, T.E. 1990. Molecular biology and biochemistry of pyruvate dehydrogenase complexes. *FASEB J.* **4**: 3224–3233.
- Pearce, K.H., Jr, Ultsch, M.H., Kelly, R.F., de Vos, A.M., and Wells, J.A. 1996. Structural and mutational analysis of affinity-inert contact residues at the growth hormone-receptor interface. *Biochemistry* **35**: 10300–10307.
- Perham, R.N. 2000. Swinging arms and swinging domains in multifunctional enzymes: Catalytic machines for multistep reactions. *Annu. Rev. Biochem.* **69**: 961–1004.
- Quioco, F.A., Wilson, D.K., and Vyas, N.K. 1989. Substrate specificity and affinity of a protein modulated by bound water molecules. *Nature* **340**: 404–407.
- Raman, C.S., Allen, M.J., and Nall, B.T. 1995. Enthalpy of antibody–cytochrome c binding. *Biochemistry* **34**: 5831–5838.
- Reed, L.J. and Hackert, M.L. 1990. Structure–function relationships in dihydrolipoamide acyltransferases. *J. Biol. Chem.* **265**: 8971–8974.
- Robien, M.A., Clore, G.M., Omichinski, J.G., Perham, R.N., Appella, E., Sakaguchi, K., and Gronenborn, A.M. 1992. Structure of the E3-binding domain of the dihydrolipoamide succinyltransferase core from the 2-oxoglutarate dehydrogenase multienzyme complex of *Escherichia coli*. *Biochemistry* **31**: 3463–3471.
- Sanderson, S.J., Miller, C., and Lindsay, J.G. 1996. Stoichiometry, organization and catalytic function of protein-X of the pyruvate dehydrogenase complex from bovine heart. *Eur. J. Biochem.* **236**: 68–77.
- Spolar, R.S., Livingstone, J.R., and Record, M.T. 1992. Use of liquid-hydrocarbon and amide transfer data to estimate contributions to thermodynamic functions of protein folding from the removal of nonpolar and polar surface from water. *Biochemistry* **31**: 3947–3955.
- Stepp, L.R. and Reed, L. J. 1985. Active-site modification of mammalian pyruvate dehydrogenase by pyridoxal 5'-phosphate. *Biochemistry* **24**: 7187–7191.
- Stites W.E. 1997. Protein–protein interactions: Interface structure, binding thermodynamics, and mutational analysis. *Chem. Rev.* **97**: 1233–1250.
- Studier, F.W., Rosenberg, A.H., Dunn, J.J., and Dubendorff, J.W. 1990. Use of T7 RNA polymerase to direct expression of cloned genes. *Methods Enzymol.* **185**: 60–89.
- Tame, J.R.H., Murshudov, G.N., Dodson, E.J., Neil, T.K., Dodson, G.G., Higgins, C.F., and Wilkinson, A.J. 1994. The structural basis of sequence-independent peptide binding by OppA. *Science* **264**: 1578–1581.
- Velazquez-Campoy, A., Todd, M. J., and Freire, E. 2000. HIV-1 protease inhibitors: Enthalpic versus entropic optimization of the binding affinity. *Biochemistry* **39**: 2201–2207.
- Wiseman, T, Williston, S., Brandts, J.F., and Nin, L-N. 1989. Rapid measurement of binding constants and heat of binding using a new titration calorimeter. *Anal. Biochem.* **179**: 131–137.